

Dynamic micro-air-bubble drifted in a liquid core fiber Fabry-Pérot interferometer for directional fiber-optic level meter

Cheng-Ling Lee, Yang-Chen Zheng, Chia-Lien Ma, Han-Jung Chang, and Chung-Fen Lee

Citation: [Applied Physics Letters](#) **102**, 193504 (2013); doi: 10.1063/1.4804992

View online: <http://dx.doi.org/10.1063/1.4804992>

View Table of Contents: <http://scitation.aip.org/content/aip/journal/apl/102/19?ver=pdfcov>

Published by the [AIP Publishing](#)

Articles you may be interested in

[Magnetic field sensing based on magneto-volume variation of magnetic fluids investigated by air-gap Fabry-Pérot fiber interferometers](#)

Appl. Phys. Lett. **103**, 111907 (2013); 10.1063/1.4821104

[Adiabatic fiber microtaper with incorporated an air-gap microcavity fiber Fabry-Pérot interferometer](#)

Appl. Phys. Lett. **103**, 033515 (2013); 10.1063/1.4815994

[A Fabry-Pérot fiber-optic ultrasonic hydrophone for the simultaneous measurement of temperature and acoustic pressure](#)

J. Acoust. Soc. Am. **125**, 3611 (2009); 10.1121/1.3117437

[Asymmetric Fabry-Pérot fiber-optic pressure sensor for liquid-level measurement](#)

Rev. Sci. Instrum. **80**, 033104 (2009); 10.1063/1.3093808

[Broadband precision wavelength meter based on a stepping Fabry-Pérot interferometer](#)

Rev. Sci. Instrum. **75**, 3318 (2004); 10.1063/1.1791871

The logo for Applied Physics Letters (AIP) is displayed in a white font on an orange background. The letters 'AIP' are large and bold, followed by a vertical bar and the words 'Applied Physics Letters' in a smaller font.

Meet The New Deputy Editors



Alexander A.
Balandin



Qing Hu



David L.
Price

Dynamic micro-air-bubble drifted in a liquid core fiber Fabry-Pérot interferometer for directional fiber-optic level meter

Cheng-Ling Lee,^{a)} Yang-Chen Zheng, Chia-Lien Ma, Han-Jung Chang, and Chung-Fen Lee
Department of Electro-Optical Engineering, National United University, Miaoli 360, Taiwan

(Received 11 April 2013; accepted 29 April 2013; published online 13 May 2013)

We propose a dynamic, directional, and miniature fiber-optic level meter based on a micro-air-bubble drifted in a liquid-core fiber Fabry-Pérot interferometer. The proposed in-fiber level meter can detect the non-horizontal/horizontal state of an object/structure and also be able to discriminate the test structure inclining to the clockwise or counterclockwise directions by measuring the spectral responses of the proposed optical fiber device. Dynamic drifting of the micro air bubble in the tilted condition has been recorded which investigates the drifted directions correlated closely with the tilted directions in the fiber level meter. © 2013 AIP Publishing LLC. [<http://dx.doi.org/10.1063/1.4804992>]

Level meter is utilized to monitor the accuracy level of the structure which is an extremely important and practical application especially useful in structure (architecture) engineering and mechanical technology. In the architecture application, the accuracy level of a construction and building is mainly concerned to the detriment of life security. Moreover, in mechanical industry, the degree of the level for mechanical elements (components) directly affects the machining accuracy and the fabricated product quality. Thus, to develop an appropriate device to monitor the level status is an urgent work. Also, together with the advantages of the optical fibers, i.e., low cost, small size, chemical stability, light weight, corrosion-resistant, and anti-electromagnetic interference, the fibers are especially suitable for effectively manufacturing many kinds of fiber devices for the fiber-optic sensing applications. Therefore, utilizing the optical fibers to develop the miniature fiber-optic level sensors is a very attractive work since such small fiber devices can be very easily embedded/attached into/onto the constructions and machines for the in-line monitoring level status immediately. However, such the fiber-optic type level meter almost has not been proposed so far even the technology of the level measurement is so imperative. Thus, in this study, we proposed a dynamic, miniature, and directional fiber-optic level meter based on a micro-air-bubble drifted in a liquid core fiber Fabry-Pérot interferometer (LC-FFPI). Many well known FFPIs have been proposed and widely applied on many physical parametric sensing,¹⁻⁷ e.g., external refractive index (RI),^{1,7} strain,²⁻⁴ and ambient temperature (T)^{1,5,6} measurements to investigate the sensitive and practical of the FFPIs. Among the above studies, a new structure of air-gap FFPIs with ellipsoidal or spherical cavity with air bubble (gap) types by special fusion splicing techniques have been reported and also shows the new characteristics and good performances on the optical Fabry-Pérot (F-P) interference.¹⁻⁴ However, the above mentioned ellipsoidal or spherical air bubbles formed in the fiber devices are fixed and immobile. The air bubbles are not able to drift correlated with the fiber directions.

Therefore, this study devotes a dynamic FFPI sensor which is based on a micro-air-bubble drifting in a liquid core

fiber for the level sensing. The spherical air bubble in our fiber sensor is movable and correlated with the level state which enables sensing of the level conditions. From the dynamic movement of the drifted air bubble, we can detect a non-horizontal/horizontal state of a structure/object and also be able to discriminate the tested structure inclining to the clockwise or counterclockwise directions when the related spectral response to be measured.

In the experiment, a single mode fiber (SMF-28) was firstly spliced a hollow core fiber (HCF) with diameter of $D = 50 \mu\text{m}$ and length L of about several hundreds of micrometers by using fusion splicing method. Then, endface of the HCF was filled with Cargille[®] optical liquid of $RI n_D = 1.4$ by duration of the capillary action. The front section of the HCF near SMF remained of air was gradually formed an air bubble during the capillary process. This is the intermolecular cohesion force of the liquid forces the trapped air to form an air bubble in the HCF. Promptly, the endface of the HCF was sealed off twice separately by a waterproof epoxy to close the fiber sensor end. Generally, due to the Marangoni effect, a globule of air (gas) in a liquid may remain intact and form into globular shape. Here the filled liquid with low viscosity coefficient is a quite good candidate since it is dilute enough to drift the air bubble for enhancing the response time. The trapped air bubble with the size of around $d_{\text{air}} \sim 46 \mu\text{m}$ (approaches to the size of the hollow core) surrounded around the filled liquid would wander around the middle of the liquid HCF when the test structure is under the almost equilibrated level (horizontal state), as shown in Fig. 1(b). On the other hand, the air bubble would drift to either left side (clockwise inclination: $-\theta$ tilted) or right side (counterclockwise inclination: $+\theta$ tilted) when the tested sensor is tilted to $-\theta$ or $+\theta$, respectively, shown in Figs. 1(a) and 1(c). Here, θ is suitable for any tilted angle. No matter what the angle is, the air bubble eventually floats to the SMF side for the $-\theta$ tilted and to the HCF end for the $+\theta$ tilted conditions. The only difference is the drifting time in different tilted angle. In Fig. 1, the d_{air} denotes the length of the air-bubble cavity, and d_{liquid} is the liquid cavities those distance is from the splicing junction of SMF/HCF to the edge of the air bubble. Here r_f and r_s generally denote the Fresnel reflections of the first and the second interfaces of the local F-P cavity, respectively. Thus, in the

^{a)}Email: cherry@nuu.edu.tw

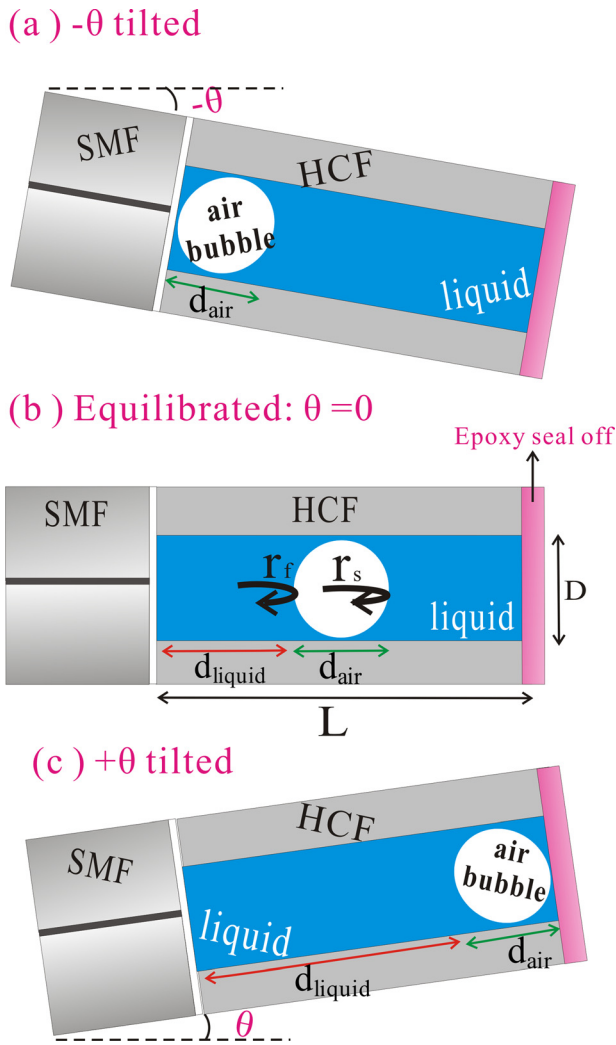


FIG. 1. Structural schematic of eventual positions of air bubbles in the proposed directional fiber-optic level meter when the conditions are (a) clockwise inclination ($-\theta$ tilted), (b) equilibrated ($\theta = 0$), and (c) counterclockwise inclination ($+\theta$ tilted), respectively.

case of $-\theta$ tilted of the sensor shown in Fig. 1(a), the length of d_{liquid} can be regarded as 0. For another far situation of $+\theta$ tilted condition, the air bubble finally drifts to the endface of the HCF where the d_{liquid} is the longest length and almost equals to $(L-d_{\text{air}})$. It can be imaged that the drifted air bubble would float and remain at the HCF endface all the time until the level direction changes. So, the position of the air-bubble in the HCF strongly depends on the degrees of horizontal level of the sensor. It is also not difficult to understand that if the fiber level meter is under the perfectly equilibrated level (horizontal state), the bubble would stay around in a midway position of the liquid HCF, as shown in Fig. 1(b). Thus the structure of the proposed LC-FFPI performs hybrid cavity which is combines a liquid cavity with almost half-length ($\sim(L-d_{\text{air}})/2$) and an air-bubble cavity with length of d_{air} . It is hard to generate the harmonic beating since the phase and frequency from the two cavities are so different. Therefore, we can simply analyze the spectral response of the LC-FFPI with the multiple F-P cavities which are mainly superimposed by the corresponding interference intensities of each F-P cavity.

Figure 2 shows reflection spectra of the interference patterns when the level status of sensor was respectively in

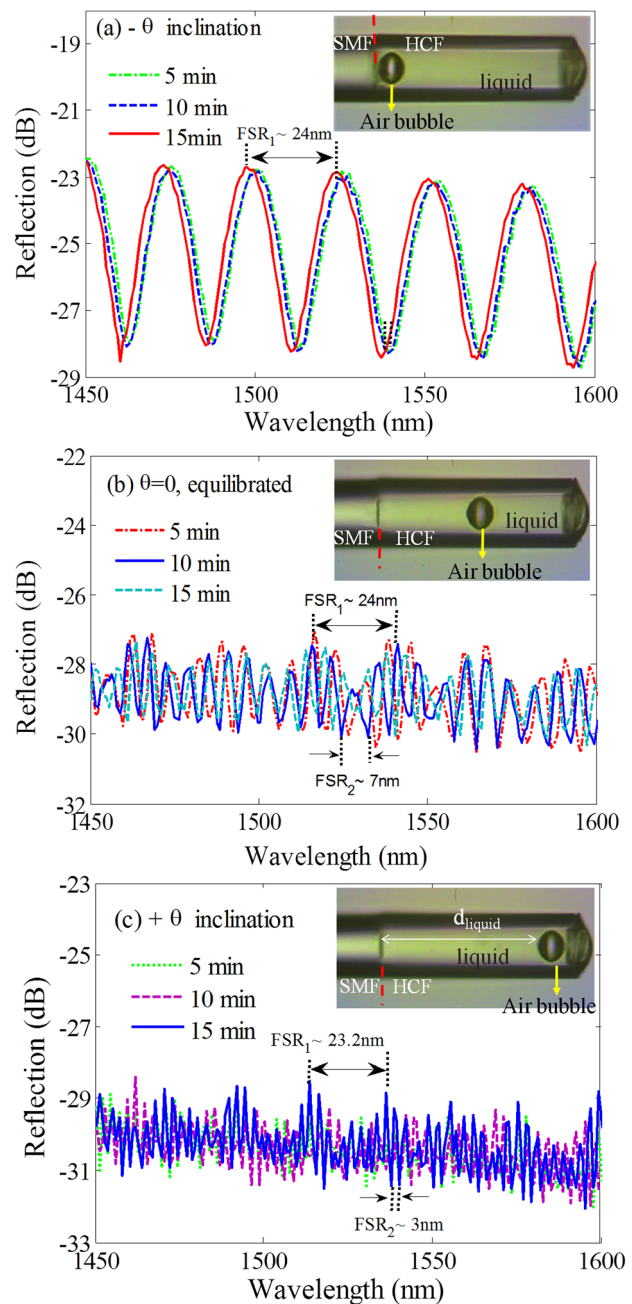


FIG. 2. Spectral responses of the measurements with different inclinations for the proposed level meters in the (a) equilibrated, (b) $-\theta$ inclination, and (c) $+\theta$ inclination conditions. Insets respectively indicate micrographs of the locations of the air-bubble in the HCFs (spectral resolution: 0.8 nm).

those cases of Fig. 1 when surrounding temperature is fixed at $T = 25^\circ\text{C}$. In Fig. 2(a), a specific condition of $-\theta$ tilted, one can see that the result performs a quasi-sinusoidal spectral response of the low finesse Fabry-Pérot interference. The loss of the optical spectrum is around 22 dB. However, it displays a relatively good interference contrast of about 5–6 dB and an almost pure sinusoidal spectra with free spectral range (FSR) of about 24 nm, named FSR_1 . Because the sensor with certain tilted angle of $-\theta$, no matter what the angle is, the air bubble finally approaches to the SMF side and thus almost fixed in the interface of SMF/HCF which can achieve a good interference pattern with a relatively smaller loss due to neglecting the liquid cavity d_{liquid} .

When the proposed level meter in the equilibrant state, optical spectra are measured and shown in Fig. 2(b). A denser interference pattern (FSR of 7 nm) with an additional enveloped modulation (around 24 nm) estimates that the air bubble drifted around the middle of the liquid HCF. The spectrum is formed by overlapping the interference intensities of the air bubble and half-path of liquid cavities. The high density of the sinusoidal pattern is from the liquid F-P interference (denoted as FSR₂), and the enveloped modulation with larger FSR₁ of around 24 nm comes from the air bubble F-P interference. Moreover, in the condition of $+\theta$ angle inclination, the air bubble always moves to the direction of the HCF end and then remains at the end position eventually at any tilted angle θ . Similarly, long liquid cavity results in a very dense interference spectrum with an almost the same amplitude modulation with period of about 23.2 nm (\sim FSR₁) as those in the case of $\theta=0$ as displayed in Fig. 2(c). Specially, in this condition of $+\theta$, the spectrum suffers a higher loss, poor extinction ratio (ER), as well as the interference possesses the narrowest FSR₂ and low contrast fringes. Therefore, it is clear to see that the optical spectra of the three cases in Fig. 2 are very different in the horizontal and non-horizontal states. Fig. 2 also further investigates the stability of the air bubble in the sensor when it was placed in the different tilted conditions (the three cases in Fig. 1) for a longer time. Figs. 2(a)–2(c), respectively, plots the interference patterns of the above three cases in many times measurements for 15 min. Insets, respectively, show the corresponding positions of the air bubble in the different inclinations. The results demonstrate that types of the spectral profiles are almost the same except a little phase deviation due to the air bubble floating. Even so, the three cases of the optical spectra can be clearly recognized and also estimates the non-horizontal state of the sensor. It is worth to mentioned, in Fig. 2(c), the optical spectra are much more variation than that of the two cases in Fig. 2(a) of $-\theta$ and Fig. 2(b) of $\theta=0$ during the 15 min. We deduce that if liquid meets slightly non-smooth surface of the epoxy seal off, it would generate the liquid flow eddied around the epoxy wall. It would make the air bubble floating more but the air bubble still stays at the HCF end. Moreover, the values of the FSR₁ and FSR₂ in the optical spectra are almost not affected which still can determine the situation of the sensor. However, we believe that there would be other suitable material of the seal off for reducing the effect of fluidic turbulence. The measurements of the spectral responses are simply analyzed as below. In the case of Fig. 2(a), the air bubble cavity dominates the interference mechanism since the power in the latter liquid cavity is so weak that is ignored. The free spectral range (FSR₁) of the air bubble cavity is expressed as below

$$\text{FSR}_1 = \frac{\lambda_1 \lambda_2}{2d_{\text{air}}}. \quad (1)$$

Here the λ_1 and λ_2 are the wavelength corresponding to the two adjacent interference peaks or dips of the reflection. Based on the FSR₁ of 24 nm measured in the spectra, the air bubble cavity d_{air} can be readily determined as 46.8 μm by using Eq. (1). In addition, the other two cases have the liquid

F-P cavities in front of the air-bubble display the high dense of FSR₂ in the responses and is shown as the following equation:

$$\text{FSR}_2 = \frac{\lambda_1 \lambda_2}{2nd_{\text{liquid}}}, \quad (2)$$

where n is the refractive index of liquid. By measuring the FSR₂ in the spectra, one can estimate the locations of the air-bubble with time varying to evaluate the dynamic vector of the air bubble as well as variations of inclination of the level meter.

In principle, in our proposed hybrid F-P structures, the reflective signal are rigorously considering as the four beam interferences which is schematically shown in Fig. 3 below. Therefore, the effective reflection of the hybrid F-P cavities can be numerically analyzed by using the ray-transfer-matrix method presented in Ref. 7 and further developing the following equation for our device:

$$\begin{aligned} I(\lambda) = & r_1 + r_2 + r_3 + r_4 + 2\sqrt{r_1 r_2} \cdot \cos(\phi_1) - 2\sqrt{r_2 r_3} \cdot \cos(\phi_2) \\ & - 2\sqrt{r_3 r_4} \cdot \cos(\phi_3) - 2\sqrt{r_1 r_3} \cdot \cos(\phi_1 + \phi_2) \\ & + 2\sqrt{r_2 r_4} \cdot \cos(\phi_2 + \phi_3) + 2\sqrt{r_1 r_4} \cdot \cos(\phi_1 + \phi_2 + \phi_3). \end{aligned} \quad (3)$$

Here, r_1 , r_2 , r_3 , and r_4 are, respectively, represent the Fresnel reflection of each interface. In Fig. 3, the phase difference of the corresponding F-P cavity is, respectively, denoted as ϕ_1 , ϕ_2 , and ϕ_3 where each cavity length is expressed as d_1 , d_2 , and d_3 . The d_2 equals d_{air} and almost remains constant, but d_1 and d_3 are variable if the air bubble moves. The optical phase difference of the cavity can be generally expressed as $\phi_k = 2n_k d_k$, $k = 2\pi/\lambda$ is the wavenumber with freespace wavelength of λ . Due to the high absorption and propagation losses in the liquid regions, the r_4 is very weak to be ignored. Thus the interference signal from the third cavity (d_3) is very weak and ascribed as a negligible contribution. The FSR₂ is dominated by the first liquid cavity ($d_1 \sim d_{\text{liquid}}$) and roughly equals to $\sim \lambda_1 \lambda_2 / (2nd_1)$. The detail optical spectra within the whole measurement range can be easily numerically calculated by using Eq. (3) once the propagation and absorption losses of the used liquid is known.

To evaluate the level sensing capability on the horizontal state of the sensor, dynamic drifting of the micro air bubble from originally equilibrant state $\theta=0$, respectively, to $-\theta$ and $+\theta$ inclinations are recorded readily and shown in Fig. 4. Fig. 4 shows the variations of FSR₂ respect to the location of the air bubble, i.e., the d_{liquid} . Insets display micrographs of the air bubble in the liquid core HCF shifts to the SMF side and HCF end, respectively. It also

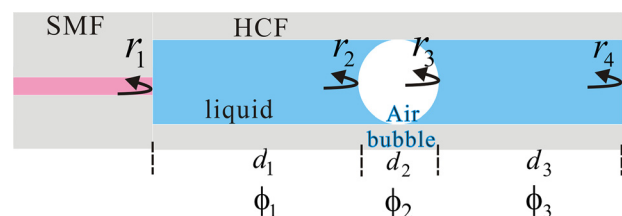


FIG. 3. Schematic diagram of the proposed sensor with hybrid F-P cavities.

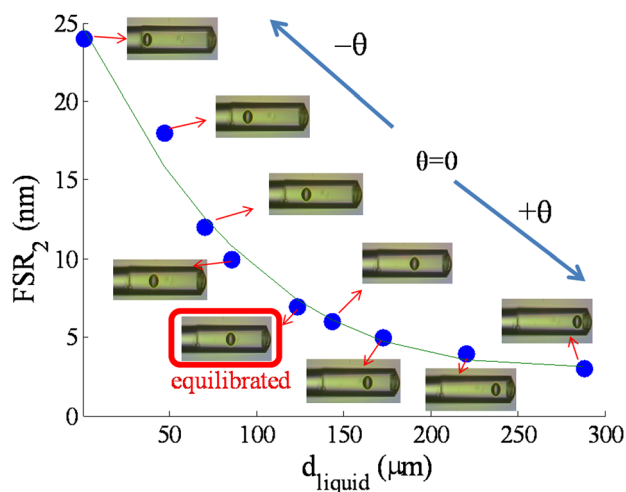


FIG. 4. Measured FSR_2 of the interference spectra with different situations (d_{liquid}). Insets show the corresponding micrographs of the air bubble locations obtained by the sensor when in the equilibrant state, respectively, tilts to SMF side ($-\theta$) and HCF end ($+\theta$) directions. Here the tilted angle θ is about 5° .

investigates the variations of the air bubble when tilted status changes. The results demonstrate that the sensor is capable of immediately monitoring the air bubble location by measuring the spectral response, especially the FSR_2 is determined quantitatively. From the dynamic results of variations in the spectral response, one can determine the inclination situations and distinguish the inclination to the clockwise or counterclockwise directions. Certainly, dynamic behaviors and response time of the drifted air bubble in the HCF are strongly affected by the tilted angles, HCF length and filling liquids. In addition, we have to admit the proposed level meter is temperature (T) sensitive since air surrounded by the liquid are easy to expand by thermal effect. To examine how the T affects spectral shifts of the optical response, the sensor (in $-\theta$ condition) is tested under a range of near room T . Figure 5 shows the T sensitivity of the sensor is high and equal to $-4.17 \text{ nm}/^\circ\text{C}$. Inset displays the wavelength shifts of the interference dips with different T . The negative sensitivity displays the spectra shift to the short wavelength region which indicates a fact: the micro air bubble in this case is compressed by the thermal effect. Generally, in a constant pressure condition, thermal expansion coefficient (TEC) of air is about $1/273 \text{ }^\circ\text{C}^{-1}$ ($+3.66 \times 10^{-3} \text{ }^\circ\text{C}^{-1}$) which is higher than that of the used liquid of $+1.0 \times 10^{-3} \text{ }^\circ\text{C}^{-1}$. However, the air/liquid is full inside a closed cavity; the volume ratio of the liquid with additional hard epoxy is much larger than that of the air. Thus, air bubble would be constricted and reduced the cavity length by the thermal effect. The T sensitive property is a drawback; however, we still think the proposed sensor can be integrated as a practical module with good temperature compensation and well calibration.

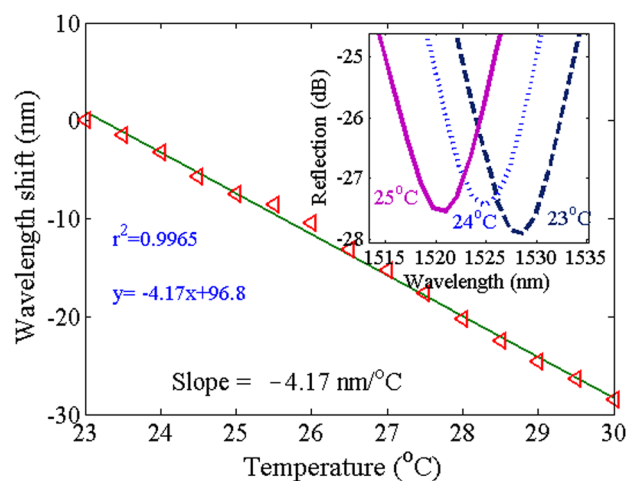


FIG. 5. Sensitivity of wavelength shift of the interference spectral dips with different temperature. Inset shows the wavelength shifts of the interference dips with different temperature.

In conclusion, we have demonstrated a dynamic, miniature and directional fiber-optic level meter based on a micro-air-bubble drifted in a liquid core fiber Fabry-Pérot interferometer. The air bubble drifted in the liquid HCF plays a sensitive and dynamic role to real-time monitor the horizontal states of the fiber level meter. From the experimental interference spectra, the proposed fiber sensor can detect the horizontal state of an object and further from the evolution of the FSR_2 in the optical spectra, the level meter also is able to distinguish the inclinations of the level meter tilted to the clockwise or counterclockwise directions. Certainly, other liquids can be utilized to improve the sensitivity and response time of the proposed sensor. It also can be expected that the level degrees would be obtained by measuring the drifted time of the micro air bubble that enables the proposed level meter to be further developed as a sensitive fiber-based angle meter.

This work was supported by the National Science Council of the Republic of China under Grant NSC 101-2221-E-239-020.

- ¹T. Wang and M. Wang, *IEEE Photon. Technol. Lett.* **24**(19), 1733–1736 (2012).
- ²E. Li, G.-D. Peng, and X. Ding, *Appl. Phys. Lett.* **92**(10), 101117–1–101117–3 (2008).
- ³D. W. Duan, Y. J. Rao, Y. S. Hou, and T. Zhu, *Appl. Opt.* **51**(8), 1033–1036 (2012).
- ⁴F. C. Favero, L. Araujo, G. Bouwmans, V. Finazzi, J. Villatoro, and V. Pruneri, *Opt. Express* **20**(7), 7112–7118 (2012).
- ⁵C. L. Lee, C. H. Hung, C. M. Li, and Y. W. You, *Opt. Commun.* **285**, 4395–4399 (2012).
- ⁶C. L. Lee, L. H. Lee, H. E. Hwang, and J. M. Hsu, *IEEE Photon. Technol. Lett.* **24**(2), 149–151 (2012).
- ⁷Y. Gong, T. Zhao, Y.-J. Rao, Y. Wu, and Y. Guo, *Opt. Express* **18**, 15844–15852 (2010).